THE s-PROCESS IN MASSIVE STARS AT LOW METALLICITY: THE EFFECT OF PRIMARY ^{14}N FROM FAST ROTATING STARS

M. PIGNATARI,[1,2] R. GALLINO,[3,4] G. MEYNET,[5] R. HIRSCHI,[1,6] F. HERWIG,[1,7] AND M. WIESCHER[2]

ABSTRACT

The goal of this Letter is to analyze the impact of a primary neutron source on the s-process nucleosynthesis in massive stars at halo metallicity. Recent stellar models including rotation at very low metallicity predict a strong production of primary ^{14}N. Part of the nitrogen produced in the H-burning shell diffuses by rotational mixing into the He core where it is converted to ^{22}Ne providing additional neutrons for the s-process. We present nucleosynthesis calculations for a 25 $M_\odot$ star at [Fe/H] = −3, −4, where about 0.8% in mass is made of primary ^{22}Ne in the convective He-burning core. The usual weak s-process shape is changed by the additional neutron source with a peak between Sr and Ba, where the s-process yields increase by orders of magnitude with respect to the yields obtained without rotation. Iron seeds are fully consumed and the maximum production of Sr, Y, and Zr is reached. On the other hand, the s-process efficiency beyond Sr and the ratio Sr/Ba are strongly affected by the amount of ^{22}Ne and by nuclear uncertainties, first of all by the ^{22}Ne$(\alpha, n)^{25}$Mg reaction. Finally, assuming that ^{22}Ne is primary in the considered metallicity range, the s-process efficiency decreases with metallicity due to the effect of the major neutron poisons ^{25}Mg and ^{22}Ne. This work represents a first step toward the study of primary neutron source effect in fast rotating massive stars, and its implications are discussed in the light of spectroscopic observations of heavy elements at halo metallicity.

Subject headings: stars: abundances — stars: chemically peculiar — stars: early-type — stars: rotation

1. INTRODUCTION

Very metal−poor halo stars have formed from matter that was only enriched by massive star ejecta (e.g., Travaglio et al. 2004). Their surface compositions thus reflect the nucleosynthesis occurring in the first generations of massive stars. A puzzling feature observed in a significant number of stars is the high Sr enrichment correlated with low Ba abundance (e.g., Truran et al. 2002; Aoki et al. 2005), with the observed Sr/Ba ratio spreading over more than 2 orders of magnitude. They are not explained by the standard r-process (rapid neutron capture process; Burbidge et al. 1957). In particular, the r-process is responsible for the production of about 20% of solar Ba and 12% of solar Sr, causing a [Sr/Ba]$_r$ = −0.22 (Sneden et al. 2008). On the other hand, stars like CS 22949−037 ([Fe/H] = −4) and the most metal−poor star known, HE 1327−2326 ([Fe/H] = −5.45), are Sr-Y rich, Ba poor, and with high [Sr/Ba] (for details see Depagne et al. 2002; Aoki et al. 2006 respectively). Another process must be responsible for the Sr observations, which is related to a similar observed Y and Zr overproduction with respect to Ba (e.g., Travaglio et al. 2004; Montes et al. 2007). Asymptotic giant branch (AGB) stars do not have time to contribute to the Galactic chemical evolution (GCE) at very low metallicity. Nor can the standard weak s-process (slow neutron capture process) in massive stars be the solution for the Sr-Y-Zr overproduction.

Indeed, the secondary nature[8] of the main neutron source ^{22}Ne progressively reduces the s-process efficiency with decreasing metallicity. In particular, for [Fe/H] ≤ −2 primary neutron poisons capture most of the neutrons causing an even faster decrease of the s-process yields with decreasing metallicity (Raiteri et al. 1992). Travaglio et al. (2004) propose that an unknown primary neutron capture process in massive stars is responsible for the production of Sr-Y-Zr, and provide an evaluation of the amount of Sr, Y, and Zr that should be produced in order to explain observations at very low metallicity: about 10% of the solar Sr and 20% of the solar Y and Zr. They called this process the light element primary process (LEPP). The unknown component could also be produced by explosive nucleosynthesis in massive stars. If in core collapse supernovae the α-rich freezeout is not complete, the final explosive nucleosynthesis in high−entropy neutrino winds from a forming neutron star may be significant for the Sr peak elements (Woosley & Hoffman 1992). More recently, Farouqi et al. (2008) and Qian & Wasserburg (2007) generally confirm the feasibility of this nucleosynthesis scenario in high-entropy neutrino winds.

Recent results from massive stars calculations at low metallicity including rotation could have important implications in this discussion. In massive stars at very low metallicity, rotation boosts the formation of primary ^{14}N. According to Meynet et al. (2006) and Hirschi (2007) due to rotational mixing primary ^{12}C produced in the convective He core is brought in contact with the bottom of the convective H shell, where it is converted into ^{14}N via the CN cycle. Part of the ^{14}N is mixed in the envelope, and part is mixed down or engulfed in the He core (e.g., Meynet et al. 2006). A more recent model by Hirschi et al. (2008) for a 20 $M_\odot$ star predicts that H-shell ashes are directly processed by the convective core He burning, causing an even higher amount of primary ^{14}N in the He core than in the previous models. During He burning, nitrogen is rapidly converted to ^{22}Ne

[1] Keele University, Keele, Staffordshire ST5 5BG, UK; marco@astro.keele.ac.uk, r.hirschi@epsam.keele.ac.uk.

[2] JINA, University of Notre Dame, Notre Dame, IN 46556; wiescher.1@nd.edu.

[3] Dipartimento di Fisica Generale, Universitá di Torino, Via Pietro Giuria 1, Torino 10125, Italy; gallino@ph.unito.it.

[4] Center for Stellar and Planetary Astrophysics, School of Mathematical Sciences, Monash University, P.O. Box 28, Victoria 3800, Australia.

[5] Geneva Observatory, CH-1290 Sauverny, Switzerland; georges.meynet@obs.unige.ch.

[6] IPMU, University of Tokyo, Kashiwa, Chiba 277-8582, Japan.

[7] Department of Physics and Astronomy, University of Victoria, Victoria, BC V8P 5C2, Canada; fherwig@uvic.ca.

[8] The production of secondary (primary) isotopes does (does not) depend on the initial metallicity of the star.
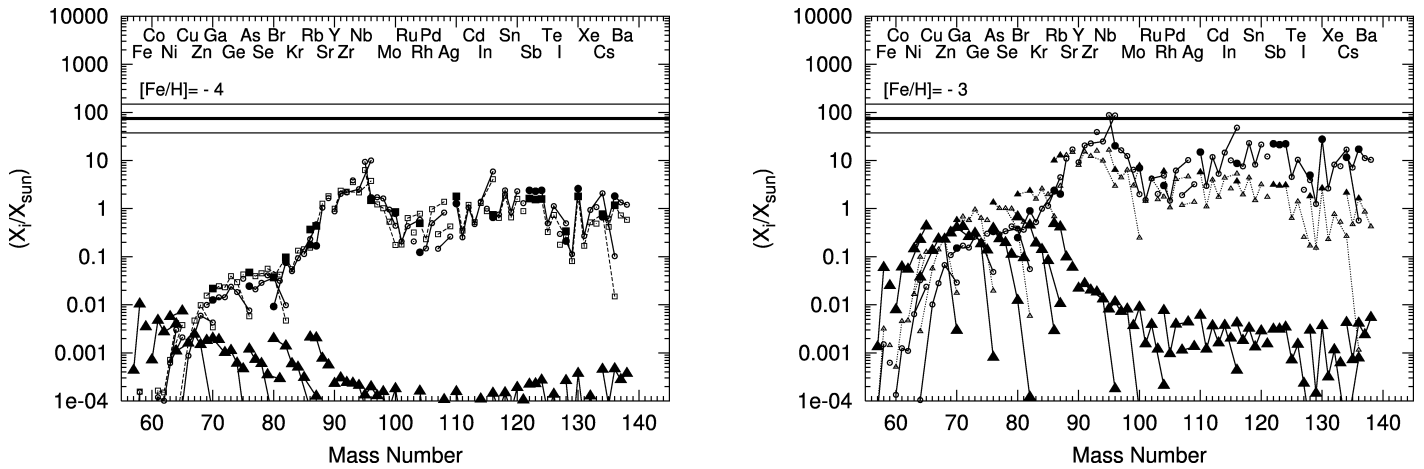
Fig. 1.—*Left*: s-process distributions between ^{57}Fe and ^{138}Ba normalized to solar for the 25 $M_\odot$ and [Fe/H] = −4 at the end of the convective C−burning shell. The horizontal lines correspond to the ^{16}O overabundance in the C shell (*thick line*), multiplied and divided by 2 (*thin lines*). Isotopes of the same element are connected by a line. The cases presented are the following: (1) standard (*black triangles*), $X(^{22}Ne)_{ini} = 5.21 \times 10^{-5}$; (2) $X(^{22}Ne)_{ini} = 5.0 \times 10^{-3}$ (*open squares*; filled squares for the s-only isotopes); (3) $X(^{22}Ne)_{ini} = 1.0 \times 10^{-2}$ (*open circles*; filled circles for the s-only isotopes). *Right*: Same as left, at [Fe/H] = −3: (1) standard (*black triangles*), $X(^{22}Ne)_{ini} = 2.12 \times 10^{-4}$; (2) $X(^{22}Ne)_{ini} = 2.0 \times 10^{-3}$ (*small triangles*); (3) $X(^{22}Ne)_{ini} = 1.0 \times 10^{-2}$ (*small circles*).

by the α-capture sequence ^{14}N$(\alpha, \gamma)^{18}$F$(\beta^+\nu)^{18}$O$(\alpha, \gamma)^{22}$Ne. Close to the He exhaustion, ^{22}Ne$(\alpha, n)^{25}$Mg is activated providing neutrons for the s-process. Hirschi et al. (2008) quantified that for a 20 $M_\odot$ star with [Fe/H] = −4.3 the primary ^{22}Ne in the He core before the s-process activation is about 0.8% in mass, about 200 times more than in the case with no rotation.

Spectroscopic observations by Spite et al. (2005) and Israelian et al. (2004) indicate a primary production of nitrogen over a large metallicity range for [Fe/H] > −4.1, and also at lower metallicities strong N enrichment has been observed in stars correlated with Sr enrichment (e.g., HE 1327−2326; Frebel et al. 2005). Chiappini et al. (2006) show that the primary nature of nitrogen can be explained at low metallicity by using the yields of fast rotating massive stars. Since the production of primary nitrogen is directly related to the ^{22}Ne available in the He core, we may also expect that the additional ^{22}Ne is produced in a primary way over a large metallicity range.

In the present work, our aim is to investigate possible consequences of massive star models including rotation on the synthesis of s-process elements. In § 2 we present s-process nucleosynthesis calculations in the He core and in the following convective C-burning shell of a 25 $M_\odot$ at [Fe/H] = −3, −4. Our final discussion and conclusions are given in § 3.

2. CALCULATIONS AND RESULTS

We present s-process calculations for a 25 $M_\odot$ star at [Fe/H] = −3, −4. A post-processing code has been used to follow the s-process in the convective He core phase and in the convective C shell phase (Raiteri et al. 1991). In particular, the C shell burns over the ashes of the previous He core. In this phase the main neutron source for neutron capture is the ^{22}Ne left after He burning. During the supernova explosion, most of the convective C shell region is ejected unchanged carrying the s-process signature of the preexplosive phase. For a 25 $M_\odot$ star, indeed, the material up to 3–3.5 $M_\odot$ is further processed and the s yields are destroyed. Between 3–3.5 $M_\odot$ and 6–6.5 $M_\odot$ the O-rich and s-process-rich material is ejected almost unchanged by the explosion (e.g., Woosley et al. 2002).

The nuclear network has been updated, as described in Pignatari et al. (2006). In particular, the ^{22}Ne$(\alpha, n)^{25}$Mg and the ^{12}C$(\alpha, \gamma)^{16}$O rates are from Jaeger et al. (2001) and from Caugh-

lan et al. (1985), respectively. In the initial composition, α-enhancements for the light isotopes are included according to Mishenina et al. (2000) for the oxygen and to Goswami & Prantzos (2000) and François et al. (2004) for the other elements. Heavy isotope abundances beyond iron are solar-scaled with the initial metallicity.

In Figure 1 (*left*) the isotopic distributions between ^{57}Fe and ^{138}Ba are presented at the end of the C-burning shell of a 25 $M_\odot$ star at [Fe/H] = −4 for three cases: (1) the standard s-process distribution, (2, 3) s-process distributions where the additional ^{22}Ne is 0.5% and 1.0% in mass (about 100 and 200 times more than in the standard case), respectively, in agreement with Hirschi et al. (2008). For each of these cases, in Table 1 the s-process parameters have been reported with the final C-shell abundances Y_i for a sample of elements. The ejected C shell mass of element i, em$_i$, is given by em$_i$ = Dm × $\bar{A_i}$ × Y_i, where $\bar{A_i}$ is the average mass number of element i and it is given in Table 1, and Dm is the C-shell mass ejected unchanged by the explosion in $M_\odot$. For comparison, the amount of ^{56}Fe produced by a 25 $M_\odot$ star is 0.1–0.2 $M_\odot$, it is primary and it strongly depends on the explosion parameters (e.g., Rauscher et al. 2002).

In case 1 the isotopic distribution is peaked between Fe and Sr. The ^{22}Ne abundance depends on the initial CNO abundances used for a given metallicity and on the α-enhancements used for light elements. As already mentioned in § 1, for [Fe/H] ≤ −2 the main neutron poisons are primary in the He core, and the probability that a free neutron is captured by iron seeds is so low that the s-process efficiency decreases more rapidly than the iron seeds with decreasing metallicity (e.g., Raiteri et al. 1992). Notice that in the C shell the s-process efficiency is strongly reduced by primary neutron poisons like ^{20}Ne and ^{23}Na (produced by the ^{12}C + ^{12}C reaction). At [Fe/H] = −4, in cases 2 and 3 iron seeds are more consumed with respect to standard s-process calculations. The s-process efficiency between Sr and Ba is increased by orders of magnitude, producing a flat isotopic pattern in this mass region. In particular, case 2 is more efficient in producing isotopes in the Pd region and less efficient in producing heavier elements with respect to case 3. On the other hand, case 2 and case 3 provide similar results for Sr, Y, and Zr (within a factor 1.3), at the bottleneck of the neutron capture flow. This implies that the Sr/Ba ratio decreases with increasing

TABLE 1
PARAMETERS

Parameter[a]	[Fe/H] = −3	[Fe/H] = −3	[Fe/H] = −3	[Fe/H] = −4	[Fe/H] = −4	[Fe/H] = −4
$X(^{22}\text{Ne})_{\text{ini}}$	2.12×10^{-4}	2.0×10^{-3}	1.0×10^{-2}	5.21×10^{-5}	5.0×10^{-3}	1.0×10^{-2}
τ (mbarn^{-1})	0.255	0.659	0.923	0.118	0.841	0.942
Heco$(n_n)_{\text{max}}$ (cm^{-3})	2.808×10^{7}	6.073×10^{7}	7.912×10^{7}	1.475×10^{7}	7.317×10^{7}	7.976×10^{7}
Csh$(n_n)_{\text{max}}$ (cm^{-3})	7.278×10^{11}	1.518×10^{12}	3.691×10^{12}	7.021×10^{11}	2.969×10^{12}	4.362×10^{12}
Sr (87.7)	9.304×10^{-11}	7.440×10^{-9}	5.595×10^{-9}	5.823×10^{-13}	6.589×10^{-10}	5.294×10^{-10}
Y (89.0)	6.964×10^{-12}	1.746×10^{-9}	1.992×10^{-9}	6.450×10^{-14}	2.130×10^{-10}	1.935×10^{-10}
Zr (91.3)	5.754×10^{-12}	2.806×10^{-9}	5.094×10^{-9}	6.623×10^{-14}	4.745×10^{-10}	5.115×10^{-10}
Mo (96.0)	3.751×10^{-13}	3.656×10^{-10}	6.885×10^{-10}	6.663×10^{-15}	1.055×10^{-10}	1.526×10^{-10}
Ba (137.4)	5.222×10^{-13}	6.917×10^{-11}	1.222×10^{-9}	3.967×10^{-14}	7.270×10^{-11}	1.378×10^{-10}

NOTES.—For the cases in Fig. 1 the neutron exposure τ, the peak central neutron density in the He core, and the peak neutron density in the C shell are reported. The initial ^{22}Ne mass fraction available in the He core and the final C shell number abundances Y_i for a sample of elements are reported, and in the first column the average mass number of element i ($\bar{A}_i$) is given in parentheses.
[a] $M = 25\ M_\odot$ for all cases.

^{22}Ne: according to Table 1, in case 2 the Sr/Ba = 9.1 and in case 3 Sr/Ba = 3.8. The addition of more primary ^{22}Ne does not imply a higher production of Sr, Y, and Zr. This happens for two main reasons. The first reason is related to the light isotope abundances. Indeed, at [Fe/H] = −4 most of the neutrons produced by ^{22}Ne are captured by the strongest neutron poisons, ^{25}Mg and ^{22}Ne (^{16}O is the strongest neutron absorber, but the neutrons are efficiently recycled via the ^{17}O(α, n)^{20}Ne reaction). The second reason is related to the *s*-process seeds. In Figure 1 (*left*) Fe seeds have been destroyed by the *s*-process, and the resulting abundances for elements between Fe and Sr are smaller than the abundances of elements beyond Sr. In case 2 of Figure 1 (*left*) the resulting *s*-process production yields for elements up to Rb (included) is less than 1% than for elements beyond it. This implies that the neutron capture nucleosynthesis flow producing Sr is exhausted.

In Figure 1 (*right*) we present similar results at [Fe/H] = −3. The corresponding *s*-process parameters and element abundances have been reported in Table 1. The new generation of models presented by Hirschi et al. (2008) does not yet include models with [Fe/H] ~ −3. However, since the nitrogen is observed to be primary over a large range of metallicity (Spite et al. 2005), we discuss now the possibility that the additional ^{22}Ne is produced with similar efficiency in the He core at [Fe/H] = −3. In Figure 1 (*right*) the isotopic distribution without additional ^{22}Ne (case 1) is similar to the isotopic distribution at solar metallicity (e.g., Rauscher et al. 2002; Pignatari et al. 2006). In

particular, a peak of production is obtained in a large mass region between Cu and Sr and with a rapid fall beyond Y, where the standard weak *s*-process is not efficient. On the other hand, the production factors in case 1 are about three orders of magnitude lower than in the case at solar metallicity, confirming the secondary nature of the weak *s*-process in massive stars. In case 2 and case 3 the primary ^{22}Ne is 0.2% and 1% in mass (about 10 and 50 times more than in the standard case with no rotation), respectively. In this case we consider a larger range of ^{22}Ne with respect to [Fe/H] = −4, to test the sensitivity of *s*-process calculations to different amounts of the neutron source. Like at [Fe/H] = −4, the mass region Fe-Zn is again substantially depleted in cases 2 and 3 with respect to case 1. On the other hand, quite similar results are observed between Zn and Kr. Finally, abundances beyond Kr are strongly enhanced in the calculations including primary ^{22}Ne. At [Fe/H] = −3 the iron seeds are a factor 10 higher than at [Fe/H] = −4, and the *s*-process efficiency increases by about a factor 10 in cases 2 and 3 with respect to similar cases in Figure 1 (*left*). As recalled above, since the neutron source ^{22}Ne and the main neutron poisons ^{25}Mg and ^{22}Ne are primary, the *s*-process is secondary scaling with the iron seed abundance. Without considering smaller local differences, the isotopic patterns at [Fe/H] = −3, −4 are quite similar. Notice that changing the primary ^{22}Ne amount by a factor of 5 affects the Sr, Y, and Zr production less than a factor of 2. Concerning heavier isotopes, more primary ^{22}Ne implies a more efficient production in the Ba region, more ^{22}Ne left in the He core ashes, and as a consequence higher neutron densities in the C shell (e.g., ^{96}Zr overproduction in case 3 with respect to case 2). In particular, in case 2 Sr/Ba = 107.6, which is strongly larger than in case 3 with Sr/Ba = 4.6.

Considering metallicities higher than [Fe/H] ~ −3 and closer to solar metallicity, rotational velocity and the related mixing efficiency in stars should decrease, assuming that stars of different metallicity begin their evolution with similar angular momentum (e.g., Meynet et al. 2006; Hirschi 2007). Therefore, the production of primary ^{14}N and of the additional ^{22}Ne in the He core becomes negligible at solar metallicity. This implies that the new *s*−process component discussed in this Letter is activated at metallicities typical of the Galactic halo, but not for metallicities of the Galactic disk.

An interesting point to discuss is how much the nuclear rates affect our results. It is well known that the ^{22}Ne(α, n)^{25}Mg reaction rate and the relative (α, n)/(α, γ) ratio affect the *s*-process nucleosynthesis. In Figure 2 we present case 3 of Figure 1 (*right*) where the ^{22}Ne(α, n)^{25}Mg recommended rate (Jaeger et al. 2001) has been multiplied and divided by a factor of 2. Elements lighter than Sr
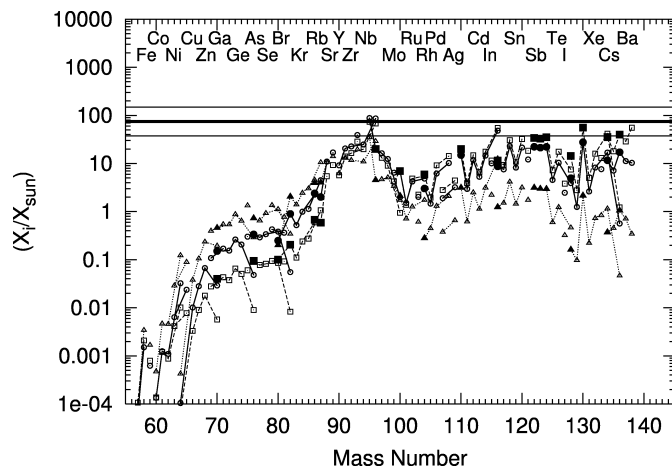

FIG. 2.—Same as case 3 in Fig. 1 (*right*), but using different ^{22}Ne(α, n)^{25}Mg rates: recommended (*circles*), recommended times 2 (*squares*), and recommended divided by 2 (*triangles*).

are more produced with a lower ^{22}Ne$(\alpha, n)^{25}$Mg rate, since fewer neutrons are available to feed heavier elements through following neutron captures. The opposite effect is observed with higher ^{22}Ne$(\alpha, n)^{25}$Mg. The higher (α, n) rate and higher $(\alpha, n)/(\alpha, \gamma)$ ratio do not strongly affect our calculations between Sr and Ba. The reason is that in this case more neutrons are produced but also more ^{25}Mg, which is the strongest neutron poison in these conditions. Furthermore, iron seeds are destroyed and cannot feed the nucleosynthesis of Sr, Y, and Zr. For instance, in case 3 of Figure 1 (*right*) the amount of material between Fe and Rb is less than 1% of the material beyond Sr. On the other hand, the *s*-process distribution beyond Sr shows a strong propagation effect due to a lower (α, n) rate. In this case, fewer neutrons and ^{25}Mg are produced but more ^{22}Ne is left, which is also a neutron poison, causing a lower *s*-process efficiency. Assuming a factor of 2 uncertainty for the ^{22}Ne$(\alpha, n)^{25}$Mg, the Sr/Ba ratio changes by a factor of 221 [0.5 and 110.4 for the $(\alpha, n) \times 2$ case and for the $(\alpha, n)/2$ case, respectively]! Out of the range of Figure 1 (*right*), the distribution beyond Ba is also significantly affected. For example, the ratio Sr/Pb ranges between 1.9 and 8059.7 for the $(\alpha, n) \times 2$ case and the $(\alpha, n)/2$ case, respectively. This large effect is due to the amount of ^{22}Ne consumed in the He core: Sr, Y, and Zr are no more produced, but heavier elements in Ba and Pb peaks are fed at the expense of lighter *s*-process isotopes. Related to this last point is also the nuclear uncertainty of ^{12}C$(\alpha, \gamma)^{16}$O, which is in competition with the ^{22}Ne$(\alpha, n)^{25}$Mg capturing helium before its exhaustion in the He core. For instance, a lower ^{12}C$(\alpha, \gamma)^{16}$O rate increases the amount of ^{22}Ne burned in the He core, and it implies a more efficient *s*-nucleosynthesis at both the Ba and the Pb peaks. Other nuclear uncertainties [e.g., the ^{16}O$(n, \gamma)^{17}$O and the ^{17}O$(\alpha, \gamma)^{21}$Ne cross sections] may also affect the calculations.

3. DISCUSSION AND FINAL REMARKS

We presented a first study of the effect of rotational mixing in massive stars on the *s*-process at [Fe/H] $= -3, -4$. A grid of models for a large spread of masses and metallicities is required for a more detailed analysis, including an evaluation of the impact of stellar model physics uncertainties. Notice also that other processes not considered in the present models may affect the mixing efficiency and the nucleosynthesis in massive stars, e.g., binary interaction and magnetic field (e.g., Langer et al. 2008).

In the calculations presented at [Fe/H] $= -3, -4$, the additional ^{22}Ne due to rotation is assumed to be primary in the He core and in the following C shell, and it causes a peak of production in the region between Sr and Ba. In this mass region the *s*-process efficiency is orders of magnitude higher than in the case with no rotation. The main neutron poisons are ^{25}Mg and ^{22}Ne. Iron seeds are strongly depleted, building up Sr-Y-Zr isotopes at the first *s*-peak at neutron magic $N = 50$. Further burning of ^{22}Ne in the He core uses the abundant Sr-Y-Zr isotopes as seeds for the production of heavier *s*-elements. The *s*-process efficiency at the Ba peak (and at the Pb peak) is affected by the amount of primary ^{22}Ne, by the fraction of ^{22}Ne burned in the He core and by nuclear uncertainties, in particular by the ^{22}Ne$(\alpha, n)^{25}$Mg and the ^{12}C$(\alpha, \gamma)^{16}$O. Indeed, the Sr/Ba ratio changes by 2 orders of magnitude considering a factor of 2 uncertainty for the ^{22}Ne$(\alpha, n)^{25}$Mg. The *s*-process in fast rotating massive stars could provide a new scenario to explain the Sr enrichment coupled with high Sr/Ba observed in many stars (Truran et al. 2002; Aoki et al. 2005) at very low metallicity, including also the spread in the observed Sr/Ba ratio. On the other hand, the *s*-process component activated by the additional ^{22}Ne due to rotation is a secondary−like process for the Sr peak elements in the range of metallicity considered, whereas the Sr enrichment is still observed in stars like HE 1327−2326 ([Fe/H] $= -5.45$). This last point could be a strong constraint to rule out this scenario. Unfortunately, elements between Zr and Ba have been observed in few metal-poor stars to constrain the signature of the proposed *s*-process mechanism. A noticeable exception is the star HD 122563 (e.g., Montes et al. 2007 and references therein), where one to two lines have been detected and measured for elements in this mass region. More observations are required to draw firm conclusions. New models at higher metallicity are necessary to study the chemical evolution of the Galactic disk. The models presented here could have important consequences for the chemical evolution of elements between Sr and Ba in the Galactic halo.

REFERENCES

Aoki, W., et al. 2005, ApJ, 632, 611
———. 2006, ApJ, 639, 897
Burbidge, E. M., Burbidge, G. R., Fowler, W. A., & Hoyle, F. 1957, Rev. Mod. Phys., 29, 347
Caughlan, G. R., Fowler, W. A., Harris, M. J., & Zimmerman, B. A. 1985, At. Data Nucl. Data Tables, 32, 197
Chiappini, C., Hirschi, R., Meynet, G., Ekström, S., Maeder, A., & Matteucci, F. 2006, A&A, 449, L27
Depagne, E., et al. 2002, A&A, 390, 187
Farouqi, K., Kratz, K.-L., Cowan, J. J., Mashonkina, L. I., Pfeiffer, B., Sneden, C., Thielemann, F.-K., & Truran, J. W. 2008, in AIP Conf. Proc. 990, First Stars III, ed. B. W. O'Shea et al. (New York: AIP), 309
François, P., Matteucci, F., Cayrel, R., Spite, M., Spite, F., & Chiappini, C. 2004, A&A, 421, 613
Frebel, A., et al. 2005, Nature, 434, 871
Goswami, A., & Prantzos, N. 2000, A&A, 359, 191
Hirschi, R. 2007, A&A, 461, 571
Hirschi, R., Chiappini, C., Meynet, G., Maeder, A., & Ekström, S. 2008, in IAU Symp. 250, Massive Stars as Cosmic Engines, ed. F. Bresolin et al. (Cambridge: Cambridge Univ. Press), 217
Israelian, G., Ecuvillon, A., Rebolo, R., García-López, R., Bonifacio, P., & Molaro, P. 2004, A&A, 421, 649

Jaeger, M., Kunz, R., Mayer, A., Hammer, J. W., Staudt, G., Kratz, K. L., & Pfeiffer, B. 2001, Phys. Rev. Lett., 87, 2501
Langer, N., Cantiello, M., Yoon, S.-C., Hunter, I., Brott, I., Lennon, D. J., de Mink, S. E., & Verheijdt, M. 2008, in IAU Symp. 250, Massive Stars as Cosmic Engines, ed. F. Bresolin et al. (Cambridge: Cambridge Univ. Press), 167
Meynet, G., Ekström, S., & Maeder, A. 2006, A&A, 447, 623
Mishenina, T. V., Korotin, S. A., Klochkova, V. G., & Panchuk, V. E. 2000, A&A, 353, 978
Montes, F., et al. 2007, ApJ, 671, 1685
Pignatari, M., Gallino, R., Baldovin, C., Wiescher, M., Herwig, F., & Heger, A. 2006, PoS, 061
Qian, Y.-Z., & Wasserburg, G. J. 2007, Phys. Rep., 442, 237
Raiteri, C. M., Busso, M., Picchio, G., & Gallino, R. 1991, ApJ, 371, 665
Raiteri, C. M., Gallino, R., & Busso, M. 1992, ApJ, 387, 263
Rauscher, T., Heger, A., Hoffman, R. D., & Woosley, S. E. 2002, ApJ, 576, 323
Sneden, C., Cowan, J. J., & Gallino, R. 2008, ARA&A, 46, 241
Spite, M., et al. 2005, A&A, 430, 655
Travaglio, C., Gallino, R., Arnone, E., Cowan, J., Jordan, F., & Sneden, C. 2004, ApJ, 601, 864
Truran, J. W., Cowan, J. J., Pilachowski, C. A., & Sneden, C. 2002, PASP, 114, 1293
Woosley, S. E., Heger, A., & Weaver, T. A. 2002, Rev. Mod. Phys., 74, 1015
Woosley, S. E., & Hoffman, R. 1992, ApJ, 395, 202